Diacylglycerol-Rich Domain Formation in Giant Stearoyl-Oleoyl Phosphatidylcholine Vesicles Driven by Phospholipase C Activity

Karin A. Riske and Hans-Günther Döbereiner
Max-Planck-Institut für Kolloidund Grenzflächenforschung, 14476 Golm, Germany

ABSTRACT   We have studied the effect of phospholipase C from *Bacillus cereus* and *Clostridium perfringens* (α-toxin) on giant stearoyl-oleoyl phosphatidylcholine (SOPC) vesicles. Enzyme activity leads to a binary mixture of SOPC and the diacylglycerol SOG, which phase separates into a SOPC-rich bilayer phase and a SOG-rich isotropic bulk-like domain embedded within the membrane, as seen directly by phase contrast microscopy. After prolonged enzymatic attack, all bilayer membranes are transformed into an isotropic pure SOG phase as characterized by fluorescence microscopy, differential scanning calorimetry, fluorescence anisotropy measurements, and small angle x-ray scattering. These domains may have biological relevance, serving as storage compartments for hydrophobic molecules and/or catalyzing cellular signaling events at their boundaries. Furthermore, in the early stages of asymmetric enzymatic attack to the external monolayer of giant vesicles, we observe a transient coupling of the second-messenger diacylglycerol to membrane spontaneous curvature, which decreases due to enzyme activity, before domain formation and final vesicle collapse occurs.

INTRODUCTION

Diacylglycerol (DAG) is a highly hydrophobic molecule that plays a key role in many biochemical pathways within the plasma membrane, the most notable one being the activation of protein kinase C (Bell, 1986). The ability of DAG to induce nonbilayer phases is of crucial importance to its biological functions (Das and Rand, 1986). DAG is produced in the cell by phospholipase C via lipid hydrolysis (Hergenrother and Martin, 2001). The initial increase in DAG levels has been associated with the activity of the phosphatidylinositol-specific phospholipase C (PI-PLC) (Galneder et al., 2001), whereas prolonged elevation in DAG concentration is caused by the phosphatidylcholine-preferring phospholipase C (PC-PLC) (Exton, 1990). Lipid/DAG mixtures have been extensively studied over the last decade and various phase diagrams have been obtained (Ortiz et al., 1988; Heimburg et al., 1992; López-García et al., 1994; Jiménez-Monreal et al., 1998). However, lipid/DAG mixtures obtained by in situ production of DAG within bilayer membranes through PLC activity can be quite different from thermodynamically fully equilibrated lipid/DAG dispersions. More specifically, vesicle aggregation and fusion have been established to occur only through the PLC-driven production of DAG, and not in lipid/DAG mixtures (Nieva et al., 1989, 1993; Burger et al., 1991). It is believed that the propensity of DAG to form nonbilayer phases favors aggregation and fusion of vesicles (Basáñez et al., 1996, 1997; Ruiz-Argüello et al., 1998).

The activity of PC-PLC toward phosphatidylcholines, as well as lipid mixtures containing other lipids, presents a lag

time, over which DAG is produced at lower hydrolysis rates, until, in most of the cases, 10 mol % of the lipid is converted into DAG. After that, there is a burst in hydrolysis rate, concomitant with vesicle aggregation and, sometimes, fusion as well. It has been proposed that the vesicle aggregation process is enhanced by the presence of DAG-rich domains (Basáñez et al., 1996), which would favor the aggregation of adjacent bilayers as well as bring structural defects to the lipid bilayer. Previous studies have not shown direct evidence of DAG-rich domains.

In the present study we show the formation of DAG-rich fluid-like bulky domains on the membrane surface due to the continuous production of stearoyl oleoyl glycerol (SOG) through the hydrolysis of stearoyl oleoyl phosphatidylglycerol (SOPC) by PLC. This is the first time that a fluid bilayer/fluid isotropic DAG phase separation within the bilayer is directly observed. Immiscibility has been reported in lipid/DAG mixtures mainly below the fluidus line, i.e., between gel lipid/DAG stoichiometric complexes C1 ($\sim$1:1) and/or C2 ($\sim$1:2) and pure lipid bilayer both in the gel and fluid state (Ortiz et al., 1988; Heimburg et al., 1992; López-García et al., 1994; Jiménez-Monreal et al., 1998). The domains we characterize are different in that they correspond to fluid/fluid immiscibility, and, we believe, occur in the form of a long-lived metastable state as a result of the in situ production of DAG within the bilayer. These domains were observed on the surface of giant unilamellar vesicles (GUVs) with a phase contrast optical microscope and their nature was characterized by differential scanning calorimetry (DSC), small angle x-ray scattering (SAXS), and fluorescence anisotropy. We have chosen the mono-unsaturated lipid SOPC, since natural DAGs mainly contain mixed chains, i.e., one saturated and one unsaturated acyl chain (Jiménez-Monreal et al., 1998; Di and Small, 1993). Moreover, the main phase transition of SOPC at 5°C does not affect experiments in the fluid phase at room temperature and above. However, we believe that the observed domain

---

formation is quite general and happens whenever PLC hydrolyzes lipid vesicles, thus locally producing DAG. We propose that these DAG-rich domains promote vesicle aggregation and fusion, by facilitating the connection of adjacent membranes. Both variants of PLC used in the present work, from *Bacillus cereus* (PLC$_{Bc}$) and from *Clostridium perfringens* (α-toxin), lead to domain formation. PLC$_{Bc}$ is believed to resemble the mammalian PLC, which is not yet purified, whereas α-toxin is the main factor in infection caused by *C. perfringens*, and produces hemolytic and necrotic effects in gas gangrene (Derewenda and Martin, 1998).

Further, we show in this paper a transient bilayer curvature response to the in situ production of the second messenger DAG (Dennis et al., 1991), occurring already at very low DAG concentrations. Obviously, this finding is biologically quite significant, since membrane curvature is known to be relevant in the activation of some enzymes, as for instance protein kinase C (Slater et al., 1994) and phosphoinositide 3-kinase (Hubner et al., 1998). For assessing membrane spontaneous curvature, we have performed a careful analysis of the shape fluctuation of giant vesicles in the presence of PLC in the external medium. When in the fluid state and with excess area, GUVs show large thermal shape fluctuations (Lipowsky and Sackmann, 1995; Seifert, 1997), which can be analyzed through quantitative video microscopy (Duwe et al., 1990; Käs and Sackmann, 1991; Faucon et al., 1989; Döbereiner et al., 1997, 2000a, 2000b). The fluctuation spectrum and the vesicle shape are indicative of the elastic properties of the membrane, such as the bending modulus and the spontaneous curvature. These material parameters are highly dependent on membrane composition and changes in the environment. Thus, (bio-) chemical reactions taking place at the membrane surface of a giant vesicle can be easily monitored via the resulting signatures in the fluctuation spectrum (Petrov et al., 1999; Döbereiner et al., 2003).

One of the first studies on the effect of lipases on giant vesicles (Wick et al., 1996) was carried out by applying a large local concentration of phospholipase A$_2$ (PLA$_2$) to the external surface of a vesicle or microinjecting the enzyme into the vesicle interior. PLA$_2$ caused vesicles to burst (Honger et al., 1997) when acting on the external vesicle surface, and vesicle shrinking when injected. Sphingomyelinase, which converts sphingomyelin into ceramide, was shown to induce domain formation and budding to the interior of giant vesicles (Holopainen et al., 2000; Nurminen et al., 2002). The effect of PLC$_{Bc}$ on giant SOPC vesicles was first studied by Holopainen et al. (2002). They reported a series of stepwise shrinkages of electroformed GUVs after injection of PLC$_{Bc}$ to the external medium. We extend this work and show that in situ production of DAG in the bilayer membrane first leads to a transient change in membrane curvature, and eventually phase separates into isotropic fluid bulky domains.

MATERIALS AND METHODS

Materials

SOPC (1-stearoyl-2-oleoyl-*sn*-glycero-3-phosphocholine) and the fluorescent lipid DPPE-NBD (ammonium salt of 1,2-dipalmitoyl-*sn*-glycerol-3-phosphoethanolamine-N-(7-nitro-2-1,3-benzoxadiazol-4-yl)) were purchased from Avanti Polar Lipids (Alabaster, AL). Phospholipase C from *B. cereus* was from Fluka (Steinheim, Switzerland) and phospholipase C from *C. perfringens* (α-toxin) was from Sigma (St. Louis, MO). Both enzymes were used without further purification. The fluorescent probe DPH (1,6-diphenyl-1,3,5-hexatryene) was purchased from Molecular Probes (Eugene, OR). The buffer system used was 10 mM HEPES (4-(2-hydroxyethyl)-1-piperizineethanesulfonic acid) adjusted with NaOH to pH 7.4.

Methods

Giant vesicles preparation

A chloroform SOPC solution (2 mg/ml) was spread on the rough side of a Teflon disc, which stayed under reduced pressure overnight to remove all traces of organic solvent. The Teflon plate was placed inside a glass bottle, with the rough side containing the lipid film facing up. In a prehydration step, the bottle was left in a humid atmosphere for 4 h at 37°C. Then, 4 ml of 10 mM HEPES pH 7.4 + 100 mM sucrose were gently poured inside the bottle, which was closed and left at 37°C for one or two days. After this step, a white cloud composed of the swollen giant vesicles appeared. This cloud was transferred and diluted into a solution of 10 mM HEPES pH 7.4 + 100 mM glucose. This created a sugar asymmetry between the inside and the outside of the vesicles, but no osmotic stress, since the solution osmolarity was carefully adjusted to be the same. Since sucrose solution is denser than glucose solution, the vesicles are stabilized by gravity at the bottom of the chamber allowing continuous observation (Döbereiner et al., 1997). Due to the differences in refractive index between the internal and external solution of the vesicle, the inner compartment appears darker under the phase-contrast light microscope, thus enhancing the quality of morphological analysis.

Phase-contrast microscopy

The vesicle solution was transferred into a microchamber using a micropump. The microchamber consists of a Teflon spacer sealed with a glass window on top and with a common cover slide on the bottom (Döbereiner et al., 1999). The cover slides were coated by treating them first with 3-mercaptopropyl-trimethoxysilane and then with methoxy PEG-maleimide (MW 5000), which binds to the silanized glass surface. This procedure prevented vesicle adhesion to the cover slides. The microchamber was in contact with a metal holder connected to a thermal bath, which allowed for temperature control. The external solution could be exchanged during the experiment by slowly pumping the desired solution. Visualization of the vesicles was done with an inverted Axiovert 135 Zeiss microscope equipped with a 40× Ph2 objective. Images were taken with a Hamamatsu C5985 CCD camera connected to a Vino video board of a Silicon Graphics Indy workstation. Vesicle morphology was recorded over time and could be quantified further by real time image analysis (for details, see Döbereiner et al. (1997)). Briefly, the focal plane was adjusted to include the long axis of a prolate vesicle. Choosing a coordinate system in which the x coordinate lies along the long axis of the vesicle, the vesicle equatorial contours were then represented in polar coordinates

$$R(\varphi) = R_o \left[1 + \sum_n a_n \cos(n\varphi) + b_n \sin(n\varphi) \right], \qquad (1)$$

where the angle φ was measured from the positive x axis. The time-dependent amplitudes (a_n, b_n) encode the full experimental information,

where a_2 measures vesicle ellipticity, and a_3 quantifies the degree of up/down symmetry breaking toward pear-like shapes.

Fluorescence microscopy

Giant SOPC vesicles were grown with 0.5 mol% DPPE-NBD. A monochromator Polychrome IV (T.I.L.L. Photonics GmbH, Gräfelfing, Germany) was used to excite the fluorescence at 470 nm. An optical filter separated the fluorescence emission (530 nm) from the excitation light. The fluorescence image was acquired in the same way as described above for phase contrast, but with an exposure time of 1 s.

LUVs preparation

A lipid film was formed from a chloroform solution of lipids, dried under a stream of N_2, and left under reduced pressure overnight to remove all traces of the organic solvent. Vesicles were prepared by the addition of the desired aqueous solution, followed by vortexing for ~2 min. Large unilamellar vesicles (LUVs) were obtained by extrusion (Nayar et al., 1989; Hunter and Frisken, 1998). Briefly, the vesicle dispersion was forced to pass through polycarbonate filters of 400, 200, and 100 nm several times each in descending order of their diameter. The vesicle radius was checked by dynamic light scattering to be (50 ± 15) nm.

SOPC:SOG samples

Pure SOG was obtained by treating 10 mM SOPC LUVs with a 10 U/ml PLC$_{Bc}$ in the presence of 1 mM CaCl$_2$ at 37°C overnight, leading to complete lipid hydrolysis, as confirmed by the phosphate assay described below. Chloroform was added to the end product of enzymatic reaction, so as to obtain phase separation between the chloroform phase containing the SOG and the aqueous phase, which contained the phosphatidylcholine, the enzyme, and CaCl$_2$. The chloroform phase was collected and used to form lipid films with the desired SOPC:SOG molar ratio as described above. 10 mM HEPES buffer was added to yield 1 mM total lipid concentration. The samples were vigorously vortexed overnight.

Differential scanning calorimetry

The calorimetric data were obtained with a Microcal VP instrument (Microcal, Northampton, MA). The scan rate used was 20°C/h. The sample was equilibrated for 30 min at 1°C before scanning. Baseline subtractions were performed using the Microcal DSC data analysis software.

DPH fluorescence anisotropy

A Fluorolog 3 Jobin Yvon-SPEX spectrometer was used (Jobin Yvon, Edison, NJ). Temperature was controlled by a water bath circulator. The fluorescence anisotropy of DPH was measured using $\lambda_{ex} = 367$ nm, $\lambda_{em} = 427$ nm, 2 nm slits, and 2 s acquisition time. The results shown are the average of three consecutive measurements. The error was ~3%.

Small angle x-ray scattering

CuK$_\alpha$ x rays were generated by a rotating anode Nonius FR591 and data were recorded with an image plate. The two-dimensional diffraction patterns were transformed into a one-dimensional average.

Enzyme activity

Enzyme activity was measured by quantifying the amount of phosphate from the SOPC headgroups liberated into the aqueous solution (based on Hergenrother and Martin, 1997). LUVs of 50 nm size were used. Unfortunately, enzyme kinetics could not be determined under the same conditions of the experiments performed on GUVs on the light microscope, since the lipid concentration in that case was extremely low. In addition to performing a phosphate essay, sample turbidity was employed to monitor enzyme activity. An increase in turbidity corresponds to vesicle aggregation induced by the increasing presence of diacylglycerol (Torley et al., 1994; Basáñez et al., 1996, 1997). Dynamic light scattering was used to follow the size of the aggregates with time.

RESULTS

Vesicle morphology

Single giant unilamellar SOPC vesicles were observed under a phase contrast light microscope before and after addition of phospholipase C from either *B. cereus* (PLC$_{Bc}$) or *C. perfringens* (α-toxin) to the external solution. To keep the particular vesicle under investigation in the field of view, enzyme was introduced by slowly exchanging the external solution with a micropump. Solution exchange was performed under conditions of low or vanishing activity; the whole process takes ~10 min. As the enzymes hydrolyze the SOPC lipids of the vesicle, the choline headgroups of SOPC are removed and diffuse into the aqueous buffer, whereas SOG, a diacylglycerol, is left in the bilayer.

Shown in Fig. 1 is a sequence of pictures of one vesicle after the injection of α-toxin at 25°C. After injection, the temperature was increased to 37°C. After a few minutes, a bright domain appeared on the vesicle surface, followed by a second one later on. The vesicle with the two domains remained stable for quite a long time, after which it suddenly collapsed into a single bright drop. Many vesicles showed this behavior, irrespective of detailed conditions (enzyme type and concentration, CaCl$_2$ concentration, temperature). The domains clearly extend beyond the bilayer plane. Close inspection showed that at late times, membrane domains appeared to be smoother than right after formation. In fact, the lens-like appearance points to a liquid character of these structures forming a liquid drop within the membrane. We found an average contact angle $\theta = (25 \pm 5)°$ (for the definition, see Fig. 1 *b*).

The composition and nature of these domains will be characterized in the following section.

Analyzing the moment of vesicle collapse frame by frame, we saw that collapse occurs within milliseconds after the formation of a new domain, as shown for three different vesicles in Fig. 2. At high enzyme and/or CaCl$_2$ concentrations (~1 U/ml PLC + 1 mM CaCl$_2$) the vesicles generally collapsed right after the formation of the first domain.

Both enzymes used, PLC$_{Bc}$ and α-toxin, caused the formation of these domains, which ultimately lead to vesicle collapse. The only apparent difference was that α-toxin only worked in the presence of calcium and at 37°C, whereas PLC$_{Bc}$ still significantly hydrolyzed the lipids without added calcium and at 25°C. We note here that single giant vesicles
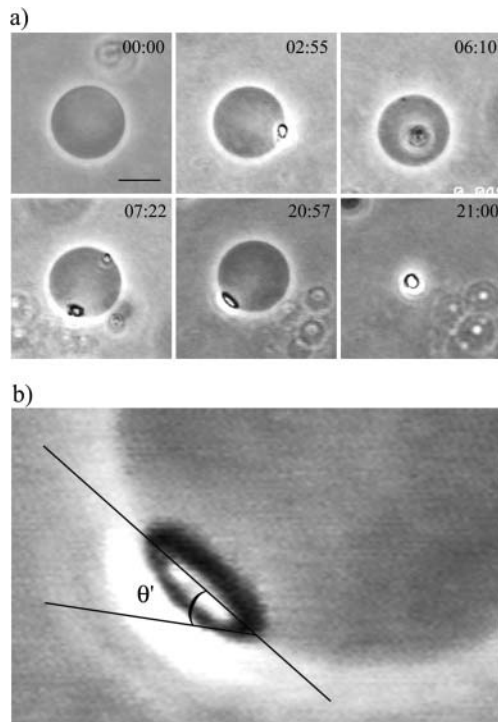
FIGURE 1 (*a*) Sequence of images of one giant SOPC vesicle in 10 mM HEPES + 100 mM sucrose/glucose (inside/outside) after the addition of 0.02 U/ml α-toxin in 0.5 mM CaCl$_2$. The enzyme solution was injected at 25°C, a temperature at which the activity of α-toxin is negligible. After that the temperature was increased to 37°C. Enzyme activity resulted in the formation of several domains. The times shown on the videographs refer to the time after the sample reached 37°C (min:s). The bar on the first image denotes 10 μm. (*b*) Apparent contact angle $\theta' = (39 \pm 4)°$ between a fluid bulky DAG-rich domain and the vesicle bilayer membrane. The equivalent contact angle θ for infinite membrane curvature radius R is somewhat smaller. In general, one finds $\theta = \theta' - \arcsin(L/2R)$ where L is the domain size. For this example, we have $\theta = (23 \pm 7)°$.

do not all follow the same enzyme kinetics, even when exposed to the same enzyme concentration. This has been observed before (Holopainen et al., 2002) and it is possibly related to the presence of small defects in the membranes, which can significantly enhance enzyme activity.

Fluorescence microscopy was used to check phospholipid partition into the bright domains. The probe used was DPPE-NBD, where the fluorescent label is attached to the headgroup of a phospholipid. Thus, if there is significant partition of phospholipids into the SOG-rich domains, they will be fluorescent. Fig. 3 *a* shows a vesicle with three domains seen by phase contrast (*left*) and fluorescence microscopy (*right*). It is clear that the fluorescent lipids are present also in these domains, which are denser than the bilayer phase. All domains on vesicles observed were fluorescent. After vesicle collapse, the remaining drops could be either fluorescent (Fig. 3 *b*) or not (Fig. 3 *c*). This implies that they turn over time into almost pure SOG.

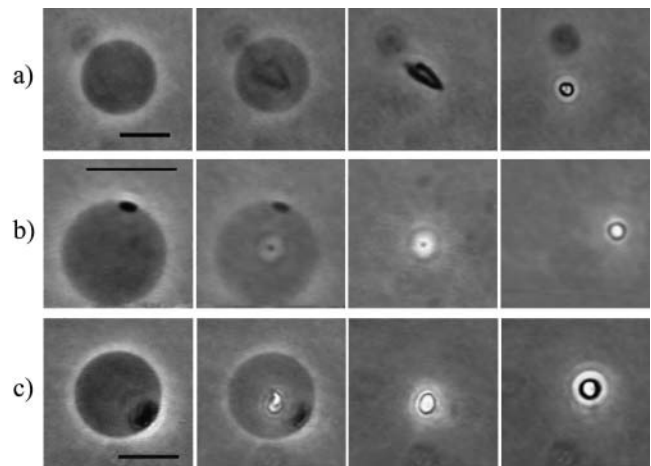A few vesicles showed a continuous shrink in diameter concomitant with the appearance of several small domains

FIGURE 2 Sequence of three different giant SOPC vesicles in 10 mM HEPES + 100 mM sucrose/glucose (inside/outside) at the moment of vesicle collapse. The first three snapshots in each row correspond to consecutive video frames (1/24 s), whereas the last snapshots were taken around 5 s after vesicle collapse. (*a*) 1 U/ml PLC$_{Bc}$, (*b*) 0.2 U/ml PLC$_{Bc}$, and (*c*) 0.5 U/ml PLC$_{Bc}$ + 1 mM CaCl$_2$. The temperature was 37°C in all cases. The same sequence of events was obtained for five more vesicles, including the one shown in Fig. 1. The scale bars denote 10 μm.

on the vesicle surface and changes in vesicle permeability, until only a drop was left. Fig. 4 *a* shows a sequence of pictures of the shrinking of one vesicle due to the action of α-toxin. The entire process occurred in <30 s ~3 h after
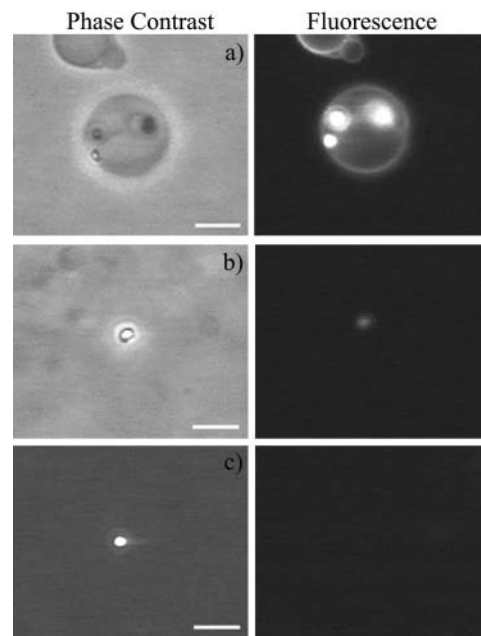

FIGURE 3 Comparison between phase contrast (*left*) and fluorescence (*right*) microscopy images. The fluorescence probe used was DPPE-NBD (0.5 mol % of the SOPC concentration). The excitation wavelength was 470 nm and emission was recorded above 520 nm. The bars denote 10 μm. (*a*) SOPC vesicle with three visible SOG-rich domains. (*b* and *c*) Two different SOG-rich drops after vesicle collapse. 10 mM HEPES + 100 mM sucrose/glucose (inside/outside) + 0.2 U/ml PLC$_{Bc}$, 37°C.
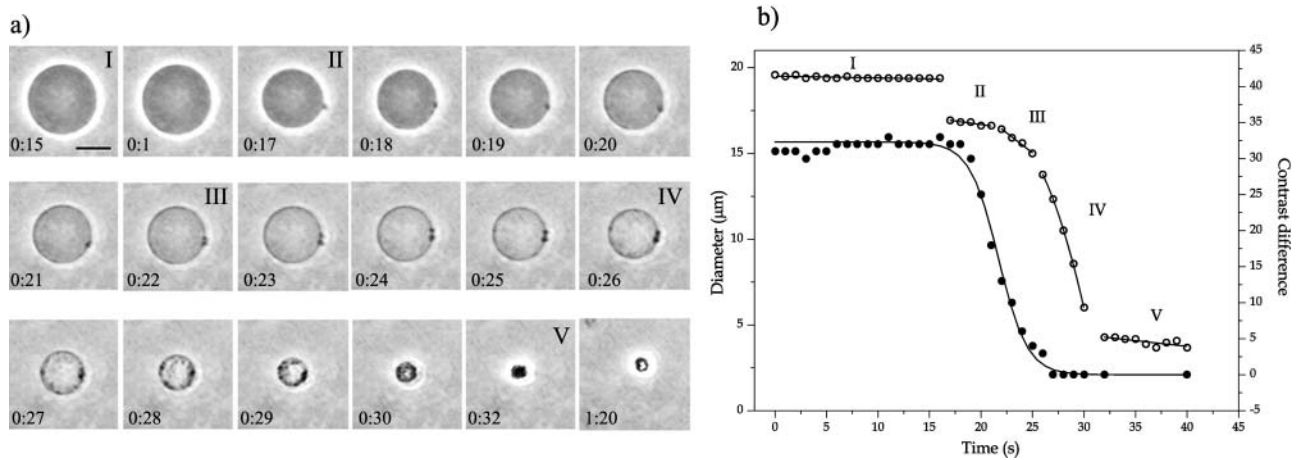
FIGURE 4   (a) Sequence of pictures of one giant SOPC vesicle after injection of 0.02 U/ml α-toxin + 0.5 mM CaCl$_2$ at 37°C. Time is set to zero at 3 h after enzyme injection, and it is shown on each figure (min:s). The bar on the first snapshot corresponds to 10 μm. 10 mM HEPES + 100 mM sucrose/glucose (inside/outside). Time intervals corresponding to the different phases of vesicle shrinkage in Fig. 5 b are denoted with Roman numbers. (b) Time dependence of vesicle diameter (*open symbols*) and contrast difference (*filled symbols*) between the inside and outside measured from the vesicle video images. There are clearly several distinct phases (for a detailed discussion, see the Appendix). Linear fits to phases I, II, III, and V are shown. A parabolic fit to phase IV serves as a guide for the eye. The decay of the contrast difference is well described by a sigmoidal curve with an exponential time constant of 1.4 s.

enzyme injection. When the first domain appeared, there was a sudden reduction in diameter, as shown in Fig. 4 b. Several domains appeared later in time, with related decreases in vesicle size. We will analyze this shrinking process in more detail in the Appendix. During shrinking, the inner vesicle compartment lost more and more of its optical contrast (Fig. 4 b), indicating formation of pores in the membrane, which lead to an exchange of sugar solution. On the other hand, the vesicle shown in Fig. 1 maintained the sugar asymmetry despite the presence of a big domain. Thus, enzyme activity does not necessarily induce vesicle leakage as has been shown in the literature (Nieva et al., 1989, 1993; Burger et al., 1991). Another morphologically similar, vesicle-shrinking process has been found with the bee venom melittin, a hemolytic peptide, when interacting with phospholipid membranes (Gerbeaud, 1998).

Our experiments were performed on a polymer-coated glass slide to avoid vesicle adhesion to the glass surface. Some early measurements were performed on uncoated glass, in which case many vesicles were adhered to the surface. As the enzymes hydrolyzed the lipids, the vesicles steadily vanished with no domain formation, and oily drops appeared on the glass surface around the vesicles (results not shown). It is quite clear that in this case, the diacylglycerol produced migrated to the glass surface.

Many authors have shown that PLC activity induces vesicles aggregation (Torley et al., 1994; Basáñez et al., 1996, 1997). We observed vesicle aggregation with LUVs (data not shown), but not with giant vesicles, due to the low lipid concentration. Yet, enzyme activity was much higher on vesicles that were clustered before enzyme injection. The conversion of part of a cluster into optically bright material
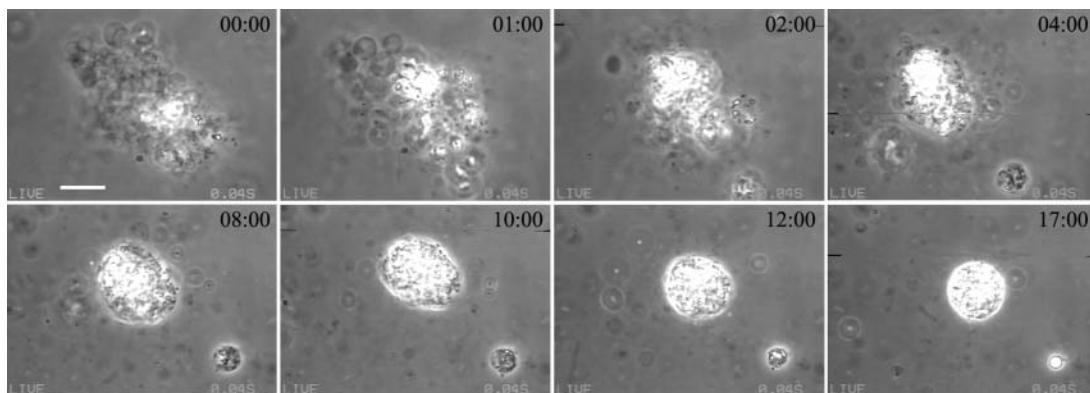

FIGURE 5   Sequence of pictures from a condensing vesicle cluster attacked by 0.5 U/ml PLC$_{Bc}$ in 1 mM CaCl$_2$ at 37°C. The first snapshot was taken ~1 h after enzyme injection. The time is written on each figure (min:s). The bar on the first image corresponds to 10 μm. A small cluster separates early on. Note the formation of two spherical compact shapes at large times, indicating fluidity of the newly formed lipid phase.

significantly increased the consumption of the rest, showing that in this case, production of SOG significantly enhanced aggregation and fusion of vesicles, as shown in Fig. 5. Note that the condensation of the highly structured vesicle cluster into a smooth spherical drop reaffirms the liquid nature of the SOG-rich phase formed by PLC activity.

Characterization of domains

The domains present on the vesicle surface are composed of a SOG-rich phase, even though SOPC is still observed in this phase through fluorescence microscopy. To define the lipid organization in these domains, we performed experiments on large unilamellar vesicles, where it is possible to tightly control vesicle size, lamellarity, and concentration. Enzyme activity on LUVs leads to an increase in sample turbidity, with a related increase in the size of scattering objects. The typical size of the reaction end product (corresponding to 70–100% lipid hydrolysis, depending on the condition) was on the order of a few hundreds of nanometers, thus, almost one order of magnitude higher than the initial LUVs size of $\sim$50 nm (data not shown and Basáñez et al., 1996). Fig. 6 *a* shows the reaction end product ($\sim$80% lipid consumption in this case) observed with phase contrast microscopy. Several bright drops ranging from 0.5 to 2 μm are observed. Comparing them with the final product obtained from giant vesicles shown in Figs. 1 and 2, it is clear that these drops are the same that develop on the membrane of giant vesicles, ultimately leading to vesicle collapse. This is also evident from the fluorescence images shown in Fig. 3.

We used differential scanning calorimetry, DPH fluorescence anisotropy and small angle x-ray scattering to further characterize the enzymatic end product shown in Fig. 6 *a*. Fig. 6 *b* shows the heat capacity (C_p) and DPH fluorescence anisotropy of the reaction end product (around 80% lipid hydrolysis) as a function of temperature. Two phase transitions at 15°C and at 20°C are seen. Above 20°C, the end product is in the melted form, as attested by the low anisotropy value, typical of a fluid phase. No transition is observed around the gel-fluid transition of pure SOPC ($T_m =$ 5°C). Comparing with data from the literature, it is clear that this thermal behavior corresponds to the one seen for hydrated SOG, which forms two different crystal phases (Di and Small, 1993): α, metastable with a melting temperature of 15°C, and β', stable but with a low nucleation rate, melting at 20°C. Similar behavior was seen for other diacylglycerols (Kodali et al., 1990). The proportion of the two crystal phases depends on the incubation time and temperature. Apart from that, dry SOG was found to exhibit five different crystal β phases, with melting temperatures all around 20°C. Some of these phases could account for the small peaks seen in Fig. 6 *b*. Thus, the temperature scan shown in Fig. 6 *b* corresponds to the melting of pure SOG. The 20 mol % SOPC that was not hydrolyzed by the enzyme should be codispersed in this diacylglycerol-rich phase.
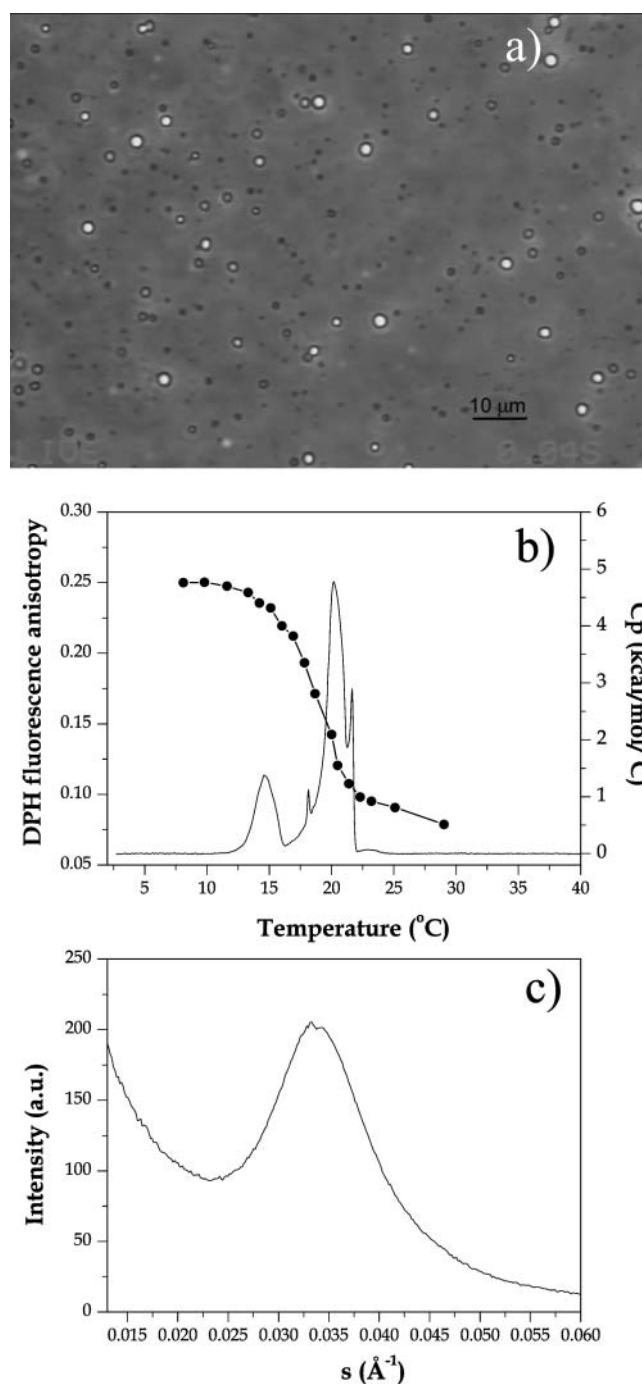

FIGURE 6 Characterization of the end product of the reaction 0.5 U/ml PLC$_{Bc}$ on 1 mM SOPC in 10 mM HEPES + 0.5 mM CaCl$_2$ for $\sim$2 h at 37°C. The total lipid consumption was $\sim$80% as measured with the phosphate assay. (*a*) A phase contrast image of reaction end product on coverslip. (*b*) Fluorescence anisotropy of 0.5 mol % DPH incorporated in SOPC before the enzymatic reaction (*connected filled symbols*) and differential scanning calorimetry (*full line*) acquired at 20°C/h (enthalpy $\Delta H = 13$ kcal/mol). (*c*) Small angle x-ray scattering acquired at 25°C. The condition for the SAXS measurements was slightly different, since much more lipid was needed for a good signal/noise ratio: 3 U/ml PLC$_{Bc}$ on 50 mM SOPC in 10 mM HEPES + 3 mM CaCl$_2$ for $\sim$2 h at 37°C
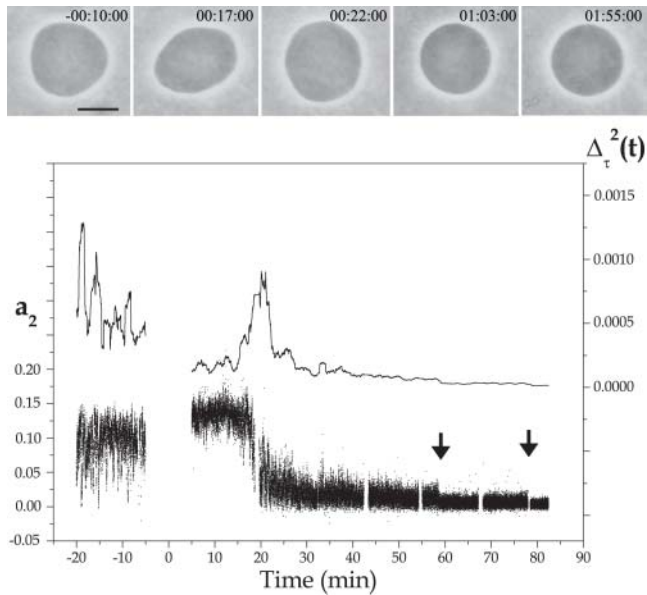
FIGURE 7 Analysis of the thermal fluctuation of SOPC GUVs in 10 mM HEPES + 100 mM sucrose/glucose (inside/outside) at 25°C in the presence of 0.2 U/ml PLC$_{Bc}$. The second fluctuation amplitude a_2 (*small dots*), which represents vesicle ellipticity, and a running-box average of width $\tau = 1$ min of the mean-square amplitude Δ_τ^2 (*full line*) are shown as a function of time. The enzyme injection takes 10 min, and no data can be acquired during the process (time zero was set to the middle of the injection process). Representative vesicle snapshots of the vesicle are shown on top. The respective times are written on the figures (h:m:s). The bar denotes 10 μm.

The SAXS results shown in Fig. 6 *c* were acquired at 25°C, thus above the phase transitions detected by DSC and fluorescence anisotropy. The broad peak centered at $q^{-1} = 30$ Å is quite different from the one observed with LUVs, where a broad peak positioned around $q^{-1} \sim 50$ Å (about the bilayer thickness) would be observed. The broad peak points to an isotropic phase.

Fluctuation spectroscopy

In the previous sections, we showed the effect of PLC on SOPC vesicles at a late stage of lipid hydrolysis, when one observes the formation of SOG-rich domains, which ultimately lead to vesicle collapse. At early stages of enzyme activity, before the formation of these bright domains, we monitored thermal shape fluctuations of GUVs. Fig. 7 shows a typical vesicle behavior before and after the addition of PLC$_{Bc}$ at 25°C. Shown in the figure are the time dependence of the fluctuation amplitude a_2, which encodes vesicle ellipticity, and its deviation from the mean $\Delta_\tau^2(t) = \langle (a_2 - \langle a_2 \rangle_\tau)^2 \rangle_\tau$ averaged over a time window of width $\tau = 1$ min. Snapshots of the vesicle at different times are shown in the top part of the figure. Before enzyme injection, the vesicle exhibits a prolate shape. It follows from the large fluctuations in a_2 that the vesicle is very close to the well-known prolate-oblate shape transition (Döbereiner and Seifert, 1996). The

corresponding vesicle snapshot shows a moment when the vesicle had a low a_2 value, almost in the oblate phase. Just after enzyme pumping, the vesicle moves away from the transition, as seen by the higher averaged a_2 value (see also snapshot on top) and by the decrease in the fluctuation amplitude $\Delta_\tau^2(t)$. This indicates an increase in the membrane spontaneous curvature and is consistent with the presence of enzymes on the surface of the external monolayer. With time, a steep decrease in a_2 with a concomitant peak in $\Delta_\tau^2(t)$ occurs, corresponding to a slow sweep of the vesicle across the prolate-oblate shape transition. In the vesicle picture on top, it is quite evident that this vesicle is in the oblate phase. We interpret this as a decrease in the membrane spontaneous curvature caused by the hydrolysis of SOPC lipids from the external vesicle monolayer. After that, the fluctuation amplitude a_2 decreases continuously with time, with a few stepwise jumps (marked with arrows in Fig. 7). This points to a decrease in vesicle excess area. The stepwise jumps coincide with the formation of small domains on the vesicle surface, though these are too small to be easily visualized on the snapshots shown on top.

In this section, we focused on variations in vesicle ellipticity induced by changes in membrane spontaneous curvature. The scenario just described was observed consistently in at least six more vesicles (results not shown). A more detailed fluctuation analysis of GUVs in the presence of PLC with a quantitative extraction of bending elastic constants is under way in our laboratory and will appear in subsequent work.

DISCUSSION

SOG-rich domains

We show in this work direct evidence of the formation of diacylglycerol-rich domains on giant lipid vesicles as a consequence of PLC activity. To our knowledge, this is the first time such a phase separation is reported and directly visualized. The domains form suddenly on the vesicle surface, and they do not necessarily induce membrane rupture and/or leakage. We observed that single vesicles can stay stable in the presence of domains for quite a long time (as seen in Fig. 1), but will ultimately collapse after the formation of a new domain, which exceeds the membrane lysis tension, as shown for three different vesicles in Fig. 2. This phase, which appears bright under phase-contrast microscopy, is mainly composed of SOG, as seen by DSC, fluorescence anisotropy, and SAXS. Above 20°C, SOG is found in the melted state as an isotropic liquid. This is easily visualized in the pictures of Fig. 1, where it is evident that the bright domain extends beyond the bilayer plane and has a liquid-like character. This domain is, in fact, a fluid drop within the bilayer, as schematically drawn in Fig. 8. The formation of such a fluid drop is a consequence of phase separation between a SOPC-rich two-dimensional bilayer
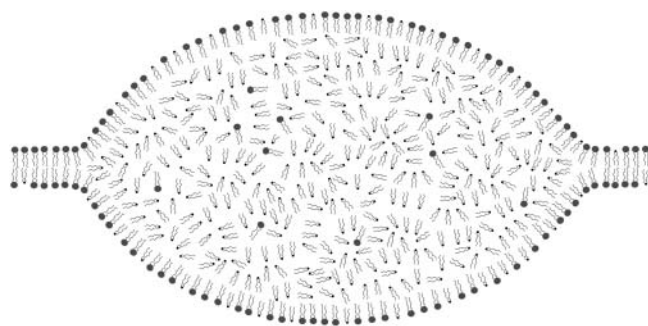
FIGURE 8 Cartoon of a SOG-rich domain coexisting with the lipid bilayer. The bilayer is rich in SOPC (drawn with bulky headgroups), whereas the lens consists of a three-dimensional liquid composed mainly of melted SOG (small headgroups), though some SOPC is certainly codispersed in this phase.

phase and a three-dimensional isotropic fluid phase rich in SOG connected to the bilayer establishing a contact angle θ of $\sim25°$. It is reasonable to assume that there will be ordered surface layers on the liquid drop consisting of SOPC and SOG, as depicted in Fig. 8, which, on a molecular scale, will join smoothly with the two monolayers of the membrane.

The contact angle θ (see Fig. 1 *b*) is determined by the balance of membrane tension σ and an effective tension σ_f exerted on the bilayer membrane (with thickness D) by the fluid drop. From dimensional arguments, the effective tension $\sigma_f = \sigma_f (p\,D,\,\sigma_s,\,\gamma/D,\,A/D^2)$ should be a function of the pressure p inside the drop, the surface tension σ_s between the drop and the bulk solution, the line tension γ along the contact line, and the Hamakar constant A, setting the van der Waals attraction between the two aqueous half spaces across the drop. However, a full analysis is beyond the scope of this paper.

The formation of the SOG-rich domains was observed only in vesicles that had not adhered to the glass surface. In experiments we performed on uncoated glass, the diacylglycerol produced in adhered vesicles migrated to the glass surface, forming oily drops. This observation explains why Holopainen et al. (2002) did not observe formation of diacylglycerol domains albeit they worked with the same lipid system. Their electroformed vesicles were still attached to the electrode, allowing the SOG to migrate to the platinum wire.

A similar drop formation has been observed to occur when toluene partitions between the bulk solution and phospholipid membranes (Brückner et al., 2000). In this case, the relative proportion of toluene to lipid is not fixed, but adjusts according to the partition equilibrium between bulk solution and the bilayer. Ultimately it is determined by the bulk concentration of toluene, when there is an excess aqueous phase. In our system, the ratio SOG:SOPC can be considered fixed. It changes adiabatically as the slow enzymatic reaction progresses. Another intercalated structure has been examined recently with lipophilic C_{60} derivatives. In contrast to

toluene, these lipo-fullerenes form rod-like aggregates in phospholipid membranes (Hetzer et al., 2000).

We stress that the DAG-rich domains reported in the present work are different from the domains observed so far in lipid/DAG equilibrated mixtures, namely the stoichiometrical lipid/DAG complexes C1 ($\sim1{:}1$) and C2 ($\sim1{:}2$) (Ortiz et al., 1988; Heimburg et al., 1992; López-García et al., 1994; Jiménez-Monreal et al., 1998). C1 and C2 complexes correspond to a gel bilayer phase, though with somewhat different structural parameters as compared to the pure phosphatidylcholine membrane (Quinn et al., 1995). Phase separation has been observed between these gel complexes and pure lipid bilayers in both gel and fluid phases. In contrast, the domains reported in this paper represent a phase separation between a fluid isotropic phase and a fluid bilayer. As verified via DSC (results not shown), our GUV experiments are performed above the melting temperatures of mixed SOPC/SOG membranes at low and high SOG content. Thus, we do not expect domain formation of solid C1/C2 complexes in these situations. However, we found a rather high melting temperature of 33°C at intermediate SOG content (40–60 mol %). Thus, at low temperatures, solid C1/C2 complexes might appear transiently as SOG content increases during enzyme activity.

From our results with giant vesicles, we could not identify at which DAG concentration domains appear. Experiments on lipid monolayers show the formation of almost pure DAG bulky domains at 25 mol % DAG, when the film is submitted to surface pressures close to the one expected for lipid bilayers (Cunningham et al., 1989). Das and Rand (1986) showed that the bilayer phase can accommodate only a limited amount of DAG, since DAG induces strong negative curvatures to the membrane monolayers. Above that limit (generally around 40–60 mol % DAG), the inverted hexagonal phase H_{II} or other nonbilayer phases are preferred (at high temperatures). However, this applies only to equilibrated mixtures where DAG is homogeneously distributed and adjacent membranes interact to form the new equilibrium bulk phase. In the case of PLC activity on single vesicles, the production of DAG occurs locally within the vesicle bilayer. Thus, due to this constraint, one expects bilayer phases to be metastable to even higher concentrations of DAG. Finally, when the DAG concentration becomes too large to be accommodated within the bilayer, phase separation of DAG-rich domains occurs. Indeed, that is what we find in our SOPC/SOG system when these fluid isotropic drops of DAG-rich phases form *embedded in* the bilayer.

Vesicle aggregation

It has been observed that PLC activity on LUVs induces vesicle aggregation (Basáñez et al., 1996, 1997), which leads to increase in sample turbidity and in aggregate size. As suggested (Basáñez et al., 1996), the vesicles cluster through

contact between some kind of DAG-rich domain in neighboring vesicles, which so far had not been identified. We propose here that the DAG-rich fluid drops observed on the surface of giant vesicles are, in fact, these domains, which trigger the process of vesicle aggregation (irrespective of size). Depending on temperature, an alternative explanation is membrane adhesion and reorganization via the well-known stalk mechanism (Kozlovsky and Kozlov, 2002) of vesicle fusion. However, in any case, C1/C2 complex domains cannot favor vesicle aggregation, since they were shown to increase the distance between adjacent lamellae (Quinn et al., 1995).

We observed aggregation of giant vesicles under the microscope in the rare cases where giant vesicles were clustered before enzyme injection, as shown in Fig. 5. In this case, it was evident that vesicle aggregation/fusion was directly linked to the formation of the DAG-rich domains on the vesicle surface. With time, the whole aggregate transformed into the DAG-rich phase. Remarkably, experiments with electron microscopy on the effect of PLC on lipid vesicles show the formation of a honeycomb structure due to the aggregation of many vesicles, which after prolonged activity, had its core transformed into an amorphous structure, proposed to be mainly pure DAG (Basáñez et al., 1997). It is clear that these electron micrographs parallel our optical microscopy sequence of events shown in Fig. 5, with the difference that under phase contrast the amorphous DAG-rich phase appears bright. For LUVs, it is reasonable to assume that the vesicles will meet more frequently so as to form clusters, due to the higher diffusion coefficient of small vesicles, and due to their higher concentration. As already suggested (Basáñez et al., 1996), the burst in activity would occur concomitant with domain formation, which would bring structural defects and the proximity of several vesicles. Our results strongly support this hypothesis. Furthermore, it seems likely that the burst in activity will never happen with single vesicles. This is because a burst requires aggregation of vesicles in addition to domain formation.

Membrane curvature response

We show in this work that fluctuation analysis of giant vesicles is a very powerful and sensitive technique to monitor chemical reactions taking place at the membrane surface, in our specific case, lipid hydrolysis by PLC. It is quite clear that even very small quantities of lipid hydrolysis products, which do not cause any visible effects on the time-averaged membrane morphology, significantly alter giant vesicle shape fluctuations. The vesicle shown in Fig. 7 exemplifies the general behavior found for many vesicles as a consequence of enzyme addition to the external solution. The cartoon in Fig. 9 illustrates our conceptual picture of the course of events during enzyme activity. The membrane is assumed in a relaxed state before enzyme interaction (a).
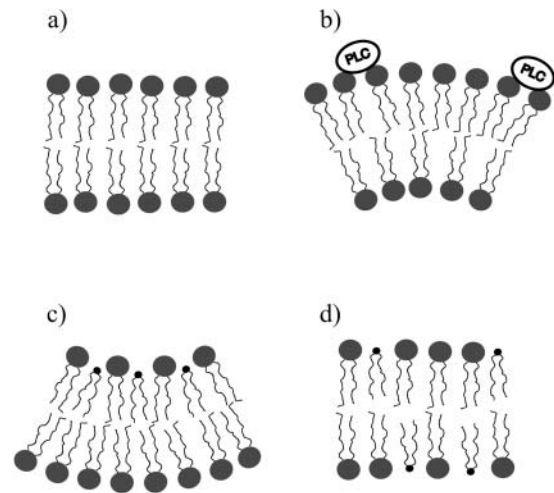

FIGURE 9 Cartoon of the effect of PLC on a relaxed lipid bilayer (a) during the first stage of the enzymatic activity. First, the adsorption of PLC molecules to the external monolayer increases the spontaneous curvature of the membrane leading to membrane bending toward the enzyme (b). Then, as SOG is produced on the external monolayer, spontaneous curvature decreases again causing reverse bending away from the enzyme (c). With time, flip-flop will occur, eventually equilibrating the SOG-produced and relaxing membrane bending (d). Formation of SOG-rich domains will ultimately occur, as schematized in Fig. 8.

Then, as the enzymes associate with the external monolayer, there is an increase in spontaneous curvature due to a decrease in surface tension of the monolayer (b), as has been observed with the addition of other molecules. As the enzymes start to work, they chemically modify the external monolayer. Since SOG induces a negative curvature to the bilayer due to its small headgroup (Leikin et al., 1996; Szule et al., 2002), a decrease in the spontaneous curvature of the bilayer is seen (c). On a longer timescale, flip-flop to the inner monolayer leads to a relaxation of bending (d). In fact, since the flip-flop rate of diacylglycerols is relatively high (60/s (Hamilton et al., 1991)), there is a steady state between SOG production on the external monolayer and lipid flip-flop to the inner monolayer. This causes immediate relaxation of most of the bilayer asymmetry, which would otherwise destroy membrane integrity. Indeed, the latter is observed with PLA_2 (Wick et al., 1996), which only modifies the hydrocarbon chains causing only small changes to flip-flop times. More precisely, if the timescale of lipid flip-flop is sufficiently faster than membrane curvature relaxation, the bilayer keeps its integrity; otherwise, disintegration occurs or, at least, a multitude of very small buds develop on the membrane. In the late stage of enzyme activity, we see a continuous decrease in overall membrane fluctuations with intervening jumps. We interpret this as a continuous loss of vesicle excess area. As discussed, the reduction at the jumps (Fig. 7) is related to the formation of new SOG-rich domains.

BIOLOGICAL IMPLICATIONS

We have established two main consecutive effects of PLC-induced DAG production in SOPC vesicles. First, asymmetric enzymatic activity on the external monolayer of a vesicle membrane leads to a transient gradient of DAG concentration across the bilayer and a corresponding decrease in spontaneous curvature inducing bending of the membrane away from the enzyme. Second, after prolonged activity, fluid domains of an isotropic DAG-rich bulk phase develop within the bilayer. Even though the present studies were carried out with model lipid vesicles composed of a single phospholipid, we believe this is a general property of PLC-driven production of DAG in lipid bilayers, since the fundamental process is the in situ production of the highly hydrophobic DAG molecule on the surface of a lipid bilayer vesicle. We note that even though DAG is a minor constituent of cell membranes (Preiss et al., 1986), it can transiently and locally reach much higher proportions, in some cases more than 10% (Wolfman and Macara, 1987). Thus, the presence of DAG-rich oil-like domains in biological membranes is quite likely. They might serve as micro storage compartments for hydrophobic substances. The special membrane boundaries between an unperturbed bilayer and the embedded oily domains could serve as activation sites of proteins involved in cell signaling (Dibble et al., 1996). Furthermore, they might be involved in cell fusion, since significant PLC activity was found in some cells where fusion events happen very often (Ribbes et al., 1987; Nieva et al., 1989). Most relevant, however, is the observed coupling of membrane curvature to the concentration and bilayer distribution of the second messenger DAG (Szule et al., 2002). It is known, for instance, that activation of protein kinase C occurs due to a transient generation of DAG within the inner leaflet of the plasma membrane (Hinderliter et al., 1997). Clearly, the coupling of a signaling event initiated by enzymatic activity to membrane morphology can serve many different functions. Such a mechanism is not restricted to the special molecular systems studied, but should have general significance (Stubbs and Slater, 1996). We note that morphological effects on the bilayer membrane and protein activation via high monolayer spontaneous curvature are not necessarily directly linked. A symmetric distribution of nonlamellar prone lipids does not lead to bilayer bending but still alters the stress distribution within the membrane, which in turn affects protein conformation.

APPENDIX: SHRINKING VESICLES

Fig. 4 shows a typical process of vesicle shrinkage after prolonged enzyme activity, which occurs in several clearly distinct phases marked with roman numbers. In phase I, the vesicle has a constant radius and shows no sign of leakage. Phase II is initiated by the formation of a domain and the opening up of a large hole in the membrane as evidenced by the sudden loss in vesicle volume. Volume loss occurs in a burst-like ejection of fluid with no diffusive exchange of sugar molecules as can be deduced from the constant vesicle contrast before and after lysis. During phase II, the vesicle radius R

diminishes with an approximately constant rate dR/dt concomitant with a strong loss in contrast. Thus, the hole(s) in the membrane do not close, but remain open with a given hole radius r, which is stable within each phase (see below). We can estimate the rate of vesicle shrinkage by equating the gain in energy ($-\sigma\, dA/dt$) as lipids, i.e., membrane area A, are incorporated into the domain at a tension level $\sigma = \sigma_f$ with the dissipation ($c\eta r v^2$) occurring during water flow through the hole. Here η is the viscosity of water, v is the mean flow velocity, and c is an unknown numerical constant of order 4π. We have

$$-\sigma\frac{d(4\pi R^2)}{dt} = nc\eta r v^2, \qquad (2)$$

where n is the number of holes in the membrane. Further, we get the velocity v by observing that the volume flow through n holes in the bilayer equals the loss in vesicle volume,

$$n\pi r^2 v = 4\pi R^2 \frac{dR}{dt},$$

$$v = 4\left(\frac{R}{r}\right)^2 \frac{dR}{dt}\frac{1}{n}. \qquad (3)$$

Inserting Eq. 3 in Eq. 2, we obtain the rate of change of the vesicle radius

$$\frac{dR}{dt} = -\frac{\pi}{2c}n\frac{\sigma r^3}{\eta}\frac{1}{R^3}. \qquad (4)$$

Assuming $q = (\pi/2c)n\sigma r^3/\eta$ to be constant, this differential equation for the radius $R(t)$ is easily solved. We find $R(t) = (R_0^4 - 4qt)^{-1/4}$, where R_0 is an integration constant, which sets the time of zero vesicle radius. However, at the late stage of vesicle shrinkage, in addition to hydrodynamic dissipation there is likely dissipation within the SOG domains as well. Thus, Eq. 2 is not valid any more. Moreover, q is not a constant but changes during shrinking. For a more refined analysis of vesicle shrinking in a somewhat different situation see Sandre et al. (1999) and Brochard-Wyart et al. (2000). In our case, we proceed with a direct analysis of the slope dR/dt. From a linear fit to the data shown in Fig. 4, we get $dR_{II}/dt = 0.1$ μm/s, which increases to $dR_{III}/dt = 0.5$ μm/s in phase III. Initially, the radius decreases only slowly and the rate is independent of the radius itself. The change in rate is correlated with the appearance of a second domain. It is unclear whether this jump is due to more holes or larger hole radii. (In fact, the tension σ should not depend on the number of domains) Nevertheless, we can estimate the hole radius in phase II by assuming just one hole. Setting σ equal to the lysis tension of SOPC, $\sigma_{lysis} = 10$ mN/m, which is mainly determined by the cohesive energy of the lipid chains, and using $\eta = 0.001$ Ns/m^2, we find with $R = 10$ μm and $c = 4\pi$ a hole radius r of $\sim$50 nm, which is a very reasonable number. In phase IV, as more and more domains develop, the decrease in vesicle radius accelerates, until the vesicle shrinking slows down abruptly in phase V, where domains from different parts of the membrane meet across the interior volume. The small continuing decrease of the vesicle radius corresponds to compactification and fusion of individual domains until a single large drop of isotropic SOG phase has formed.

REFERENCES

Basáñez, G., J.-L. Nieva, F. M. Goñi, and A. Alonso. 1996. Origin of the lag period in the phospholipase C cleavage of phospholipids in

membranes. Concomitant vesicle aggregation and enzyme activation. *Biochemistry.* 35:15183–15187.

Basáñez, G., M. B. Ruiz-Argüello, A. Alonso, F. M. Goñi, G. Karlsson, and K. Edwards. 1997. Morphological changes induced by phospholipase C and by sphingomyelinase on large unilamellar vesicle: a cryo-transmission electron microscopy study of liposome fusion. *Biophys. J.* 72:2630–2637.

Bell, R. M. 1986. Protein kinase C activation by diacylglycerol second messengers. *Cell.* 45:631–632.

Brochard-Wyart, F., P. G. de Gennes, and O. Sandre. 2000. Transient pores in stretched vesicles: role of leakout. *Physica A.* 278:32–51.

Brückner, E., P. Sonntag, and H. Rehage. 2000. Influence of toluene on the bending elastic properties of giant phosphatidylcholine vesicles. *J. Phys. Chem. B.* 104:2311–2319.

Burger, K. N. J., J.-L. Nieva, A. Alonso, and A. J. Verkleij. 1991. Phospholipase C activity-induced fusion of pure model membranes. A freeze fracture study. *Biochim. Biophys. Acta.* 1068:249–253.

Cunningham, B. A., T. Tsujita, and H. L. Brockman. 1989. Enzymatic and physical characterization of diacylglycerol-phosphatidylcholine interactions in bilayers and monolayers. *Biochemistry.* 28:32–40.

Das, S., and R. P. Rand. 1986. Modification by diacylglycerol of the structure and interaction of various phospholipid bilayer membranes. *Biochemistry.* 25:2882–2889.

Dennis, E. A., S. G. Rhee, M. M. Billah, and Y. A. Hannun. 1991. Role of phospholipases in generating lipid second messengers in signal transduction. *FASEB J.* 5:2068–2077.

Derewenda, Z. S., and T. W. Martin. 1998. Structure of the gangrene alpha-toxin: the beauty in the beast. *Nat. Struct. Biol.* 5:659–662.

Di, L., and D. M. Small. 1993. Physical behavior of the mixed chain diacylglycerol, 1-stearoyl-2-oleoyl-*sn*-glycerol: difficulties in chain packing produce marked polymorphism. *J. Lipid Res.* 34:1611–1623.

Dibble, A. R., A. K. Hinderliter, J. J. Sando, and R. L. Biltonen. 1996. Lipid lateral heterogeneity in phosphatidylcholine/phosphatidylserine/diacylglycerol vesicles and its influence on protein kinase C activation. *Biophys. J.* 71:1877–1890.

Döbereiner, H.-G. 2000a. Fluctuating vesicle shapes. *In* Giant Vesicles, Perspectives in Supramolecular Chemistry, Vol. 6. P.L. Luisi and P. Walde, editors. John Wiley & Sons, New York. 150–167.

Döbereiner, H.-G. 2000b. Properties of giant vesicles. *Curr. Opin. Colloid Interface Sci.* 5:256–263.

Döbereiner, H.-G., E. Evans, M. Kraus, U. Seifert, and M. Wortis. 1997. Mapping vesicle shapes into the phase diagram: a comparison of experiment and theory. *Phys. Rev. E.* 55:4458–4474.

Döbereiner, H.-G., P. G. Petrov, and K. A. Riske. 2003. Signatures of chemical reactions in the morphology and fluctuations of giant vesicles. *J. Phys. Cond. Matter.* 15:303–308.

Döbereiner, H.-G., and U. Seifert. 1996. Giant vesicles at the prolate-oblate transition: a macroscopic bistable system. *Europhys. Lett.* 36:325–330.

Döbereiner, H.-G., O. Selchow, and R. Lipowsky. 1999. Spontaneous curvature of fluid vesicles induced by trans-bilayer sugar asymmetry. *Eur. Biophys. J.* 28:174–178.

Duwe, H. P., J. Käs, and E. Sackmann. 1990. Bending elastic-moduli of lipid bilayers—modulation by solutes. *J. Phys. France.* 51:945–962.

Exton, J. H. 1990. Signaling through phosphatidylcholine breakdown. *J. Biol. Chem.* 265:1–4.

Faucon, J. F., M. D. Mitov, P. Meleard, I. Bivas, and P. Bothorel. 1989. Bending elasticity and thermal fluctuations of lipid-membranes—theoretical and experimental requirements. *J. Phys. France.* 50:2389–2414.

Galneder, R., V. Kahl, A. Arbuzova, M. Rebecchi, J. O. Rädler, and S. McLaughlin. 2001. Microelectrophoresis of a bilayer-coated silica bead in an optical trap: application to enzymology. *Biophys. J.* 80:2298–2309.

Gerbeaud, C. 1998. Effet de l'insertion de protéines et de peptides membranaires sur les propriétés mécaniques et les changements morphologiques de vésicules géantes. PhD thesis. Université Bordeaux 1, Talence, France.

Hamilton, J. A., S. P. Bhamidipati, D. R. Kodali, and D. M. Small. 1991. The interfacial conformation and transbilayer movement of diacylglycerols in phospholipid bilayers. *J. Biol. Chem.* 266:1177–1186.

Heimburg, T., U. Würz, and D. Marsh. 1992. Binary phase diagram of hydrated dimyristoylglycerol-dimyristoylphosphatidylcholine mixtures. *Biophys. J.* 63:1369–1378.

Hergenrother, P. J., and S. F. Martin. 1997. Determination of the kinetic parameters for phospholipase C (*Bacillus cereus*) on different phospholipid substrates using a chromogenic assay based on the quantitation of inorganic phosphate. *Anal. Biochem.* 251:45–49.

Hergenrother, P. J., and S. F. Martin. 2001. Phosphatidylcholine-preferring phospholipase C from *B. cereus*. Function, structure, and mechanism. *Top. Curr. Chem.* 211:131–167.

Hetzer, M., P. Karakatsanis, H. Casalta, A. Hirsch, X. Camps, O. Vostrowsky, and T. M. Bayerl. 2000. Diffusion and molecular dynamics of lipo-fullerenes in phospholipid membranes studied by NMR and quasi-elastic neutron scattering. *J. Phys. Chem. A.* 104:5437–5443.

Hinderliter, A. K., A. R. G. Dibble, R. L. Biltonen, and J. J. Sando. 1997. Activation of protein kinase C by coexisting diacylglycerol-enriched and diacylglycerol-poor lipid domains. *Biochemistry.* 36:6141–6148.

Holopainen, J. H., M. I. Angelova, and P. J. K. Kinnunen. 2000. Vectorial budding of vesicles by asymmetrical enzymatic formation of ceramide in giant liposomes. *Biophys. J.* 78:830–838.

Holopainen, J. M., M. I. Angelova, T. Söderlund, and P. K. J. Kinnunen. 2002. Macroscopic consequences of the action of phospholipase C on giant unilamellar liposomes. *Biophys. J.* 83:932–943.

Honger, T., K. Jorgensen, D. Stokes, R. L. Biltonen, and O. G. Mouritsen. 1997. Phospholipase A2 activity and physical properties of lipid-bilayer substrates. *Methods Enzymol.* 286:168–190.

Hubner, S., A. D. Couvillon, J. A. Käs, V. A. Bankaitis, R. Vegners, C. L. Carpenter, and P. A. Janmey. 1998. Enhancement of phosphoinositide 3-finase (PI 3-kinase) activity by membrane curvature and inositol-phospholipid-binding peptides. *Eur. J. Biochem.* 258:846–853.

Hunter, D. G., and B. J. Frisken. 1998. Effect of extrusion pressure and lipid concentration on the size and polydispersity of lipid vesicles. *Biophys. J.* 74:2996–3002.

Jiménez-Monreal, A. M., J. Villalaín, F. J. Aranda, and J. C. Gómez-Fernández. 1998. The phase behavior of aqueous dispersions of unsaturated mixtures of diacylglycerols and phospholipids. *Biochim. Biophys. Acta.* 1373:209–219.

Käs, J., and E. Sackmann. 1991. Shape transitions and shape stability of giant phospholipid-vesicles in pure water induced by area-to-volume changes. *Biophys. J.* 60:825–844.

Kodali, D. R., D. A . Fahey, and D. M. Small. 1990. Structure and polymorphism of saturated monoacid 1,2-diacyl-*sn*-glycerols. *Biochemistry.* 29:10771–10779.

Kozlovsky, Y., and M. M. Kozlov. 2002. Stalk model of membrane fusion: solution of energy crisis. *Biophys. J.* 82:882–895.

Leikin, S., M. M. Kozlov, N. L. Fuller, and R. P. Rand. 1996. Measured effect of diacylglycerol on structural and elastic properties of phospholipid membranes. *Biophys. J.* 71:2623–2632.

Lipowsky, R., and E. Sackmann. 1995. Structure and Dynamics of Membranes. Elsevier, Amsterdam.

López-García, F., J. Villalaín, J. C. Gómez-Fernández, and P. J. Quinn. 1994. The phase behavior of mixed aqueous dispersions of dipalmitoyl derivatives of phosphatidylcholine and diacylglycerol. *Biophys. J.* 66:1991–2004.

Nayar, R., M. J. Hope, and P. R. Cullis. 1989. Generation of large unilamellar vesicles from long-chain saturated phosphatidylcholines by extrusion technique. *Biochim. Biophys. Acta.* 986:200–206.

Nieva, J. L., F. M. Goñi, and A. Alonso. 1989. Liposome fusion catalytically induced by phospholipase C. *Biochemistry.* 28:7364–7367.

Nieva, J. L., F. M. Goñi, and A. Alonso. 1993. Phospholipase C-promoted membrane fusion. Retroinhibition by the end-product diacylglycerol. *Biochemistry.* 32:1054–1058.

Nurminen, T. A., J. M. Holopainen, H. Zhao, and P. K. J. Kinnunen. 2002. Observation of topological catalysis by sphingomyelinase coupled to microspheres. *J. Am. Chem. Soc.* 124:12129–12134.

Ortiz, A., J. Villalaín, and J. C. Gómez-Fernández. 1988. Interaction of diacylglycerols with phosphatidylcholine vesicles as studied by differential scanning calorimetry and fluorescent probe depolarization. *Biochemistry.* 27:9030–9036.

Petrov, P. G., J. Lee, and H.-G. Döbereiner. 1999. Coupling chemical reactions to membrane curvature: A Photochemical Morphology Switch. *Europhys. Lett.* 48:435–441.

Preiss, J., C. R. Loomis, W. R. Bishop, R. Stein, J. E. Niedel, and R. M. Bell. 1986. Quantitative measurement of *sn*-1,2-diacylglycerols present in platelets, hepatocytes, and *ras*- and *cis*-transformed normal rat kidney cells. *J. Biol. Chem.* 261:8597–8600.

Quinn, P. J., H. Takahashi, and I. Hatta. 1995. Characterization of complexes formed in fully hydrated dispersions of dipalmitoyl derivatives of phosphatidylcholine and diacylglycerol. *Biophys. J.* 68:1374–1382.

Ribbes, H., P. Monique, J. B. Pierre, C. Hugues, and D.-B. Louis. 1987. Phospholipase C from human sperm specific for phosphoinositides. *Biochim. Biophys. Acta.* 919:245–254.

Ruiz-Argüello, M. B., F. M. Goñi, and A. Alonso. 1998. Phospholipase C hydrolysis of phospholipids in bilayers of mixed lipids compositions. *Biochemistry.* 37:11621–11628.

Sandre, O., L. Moreaux, and F. Brochard-Wyart. 1999. Dynamics of transient pores in stretched vesicles. *Proc. Natl. Acad. Sci. USA.* 96:10591–10596.

Seifert, U. 1997. Configuration of fluid membranes and vesicles. *Adv. Phys.* 46:13–137.

Slater, S. J., M. B. Kelly, F. J. Taddeo, C. J. Ho, E. Rubin, and C. D. Stubbs. 1994. The modulation of protein-kinase-C activity by membrane lipid bilayer structure. *J. Biol. Chem.* 269:4866–4871.

Stubbs, C. D., and S. J. Slater. 1996. The effects of non-lamellar forming lipids on membrane protein-lipid interactions. *Chem. Phys. Lipids.* 81:185–195.

Szule, J. A., N. L. Fuller, and R. P. Rand. 2002. The effects of acyl chain length and saturation of diacylglycerols and phosphatidylcholines on membrane monolayer curvature. *Biophys. J.* 83:977–984.

Torley, L., C. Silverstrim, and W. Pickett. 1994. A turbimetric assay for phospholipase C and sphingomyelinase. *Anal. Biochem.* 222:461–464.

Wick, R., M. I. Angelova, P. Walde, and P. L. Luisi. 1996. Microinjection into giant vesicles and light microscopy investigation of enzyme-mediated vesicle transformations. *Chem. Biol.* 3:105–111.

Wolfman, A., and I. G. Macara. 1987. Elevated levels of diacylglycerol and decreased phorbol ester sensitivity in *ras*-transformed fibroblasts. *Nature.* 325:359–361.